Manuscript Preprint

Simulating Drainage from a Flooded Sinkhole[1]

Malcolm S. Field

National Center for Environmental Assessment, U.S. Environmental Protection Agency, Washington, D.C.

Abstract. Understanding sinkhole-drainage capacity and functioning is critical to realizing the effects that may be created when directing stormwater drainage to sinkholes. The importance of understanding sinkhole drainage seems to be ignored during most hydrological investigations involving sites with sinkholes in which drainage is a prime issue at site. In addition, theoretical sinkhole-drainage studies are conspicuously lacking. Sinkhole flooding often results in property damage and physical harm. In this paper, the basics of sinkhole drainage are reviewed in terms of a point vortex flow created by drainage down a sinkhole swallet. Then several different, relatively, simple sinkhole shapes are presented and mathematical models developed to simulate drainage from inflowing water. The models emphasize the significance of drainage rate as a function of sinkhole shape and sinkhole wetted cross-sectional area relative to changes in water level and time. Model simulations provide insights into the sensitivity of sinkholes to inflow rates and head changes with respect to time.

1. Introduction

Sinkholes act as natural surface-water drains, but their enhanced-use by man to control stormwater is also common. In recent years there has been some recognition of the potential risks of directing stormwater to sinkholes for drainage (e.g., risks may entail additional sinkhole development). However, recognition of the potential risks does not always translate into appropriate action. For example, recent project proposals in Lebanon County, Pennsylvania, Roanoke, Virginia, etc., still reflect attempts by developers to maximize their construction footprint by directing much, if not all of the area stormwater down one or more sinkholes at or near the property. Most such intended uses of sinkholes for stormwater drainage do not include any more than a cursory site-hydrologic evaluation.

Understanding flow processes on the surface and in the subsurface of karstic terranes is of considerable importance. Most efforts to understand surface flows use traditional hydrological methods and involve peak discharge calculations (see, for example, MDE, 2000, Appendix D.10). However, most efforts to understand subsurface flows are accomplished using a combination of typical aquifer-investigative techniques (e.g., potentiometric-surface mapping and aquifer testing), spring hydrograph assessment, and groundwater tracing from selected input points (e.g., sinking streams and sinkholes) to discharge points (e.g., springs and/or wells). Although beneficial in establishing the overall flow picture, these techniques seldom provide adequate details regarding the actual flows that occur between the input and output points. In particular, little attention seems to be directed towards sinkhole-drainage capabilities and functioning which is critical when intending to direct stormwater drainage to a sinkhole. Reese et al. (1997) briefly alludes to an assessment of sinkhole-drainage capacity, but their assessment is too limited in scope and comes across more as an afterthought than as part of an integral investigation into the drainage limits of sinkholes.

Sinkholes have been described as funnels to a water-supply line (Field, 1989). Whatever gets washed down a sinkhole also gets into the subsurface solution conduits and are eventually discharged at a downgradient resurgence if constrictions in the conduit, excessive masses, etc. do not prevent discharge. Tapping solution conduits or springs for drinking water runs the risk that materials washed into upgradient sinkholes may be harmful to human health (e.g., Fig. 1).

[1] Disclaimer: The views expressed in this paper are solely those of the author and do not necessarily reflect the views or policies of the U.S. Environmental Protection Agency.

Figure 1. Contaminant leakage from a pesticide storage warehouse into a sinkhole located in Manati, Puerto Rico. Pollutant stream is yellow in color and black sludge is built up from past releases. Photo taken during heavy precipitation is causing sinkhole to fill; one half hour after cessation of precipitation, sinkhole had completely drained.

Although the risk of dangerous substances getting washed into sinkholes is very real, it is still common practice to direct stormwater runoff into sinkholes to control flooding and to hopefully prevent additional new sinkhole occurrences. Drastically changing surface and/or subsurface hydrology tends to induce the development of new sinkholes, however. Investigations into directing stormwater drainage down a sinkhole or uvala usually entails little more than determining how to redirect surface water to the sinkhole or uvala. There is some indication, however, that local governments are now slowly moving away from directing stormwater down existing sinkholes (Parizek, 2005) and developing more comprehensive stormwater management plans specific to karst terranes (Barner, 1999). According to Fleury (2009, p. 21) stormwater management ordinances are a result of communities recognizing the need to better protect their water quality and minimize the risk of inducing new sinkholes. A not too common theme in many of the ordinances is the requirement that sinkhole-drainage capacity be determined, but finding guidance on how to make such a determination is not easily accomplished (CSN, 2009), although there are some general sources do refer to the significance of karstic terranes (see, for example, MDE, 2000; MPCA, 2008).

Sinkholes have also been described as diagnostic of karst (Quinlan, pers. comm.) and/or as the fundamental unit of karst relief (Sweeting, 1973, p. 44). That is, if you have a sinkhole, then you are in a karstic terrane. However, the reverse is not necessarily true; the absence of sinkholes does not rule-out karst (Ford and Williams, 2007, p. 339). Sinkhole occurrence, distribution, and formation have all been the subject of extensive studies for many decades (see, for example, Cvijić, 2005; Ford, 1963; Jennings, 1985; Sweeting, 1973; Williams, 1971, 1983, 1985; Gao, 2002) as have been the construction aspects of building on sinkholes (e.g., Sowers, 1996; Waltham et al., 2005). Some research efforts have also been directed towards better stormwater-quality management when intending to use sinkholes for stormwater drainage (see, for example, Crawford and Gorves, 1995; Kalmes and Mohring, 1995; Keith et al., 1995). However, little research appears to have been directed at understanding sinkhole-drainage functioning.

In an effort to obtain a better understanding of sinkhole functioning, a model for sinkhole drainage was developed and simulations conducted. The model is considered to be reasonably realistic in that it is developed with the observed occurrence of flow into and down a sinkhole of moderate-size dimensions and that is drained by a swallet. The model is limited to theoretical conditions because of, for example, the assumption of symmetry of sinkhole shape and viscosities equal to that of water. The model does not address the pressure head necessary to drive a plug down the swallet;

rather the model only balances inflow and outflow as related to instantaneous flushing of water down the swallet.

2. Sinkhole-Drainage Hydrology

Drainage down a sinkhole swallet is of particular interest to local managers when the underlying swallet becomes plugged or inflow exceeds the drainage capacity of the swallet because the sinkhole will tend to become temporarily flooded until either inflows are reduced or sufficient pressure is developed such that the plug is forced down the swallet. Waltham et al. (2005, p. 251–253) provides a brief discussion of the causes of sinkhole flooding and the need to address the problem. Zhou (2007) provides a somewhat more comprehensive discussion of the causes for sinkhole flooding and the need to recognize the importance of understanding sinkhole drainage. According to Zhou, the main causes for sinkhole flooding are (1) excessive recharge to the sinkhole, (2) excessive inflows, and (3) inadequate discharge. Soil-plugged sinkholes, which fall under the category of excessive recharge defined by Zhou, are quite common as evidenced by the example of a dropout doline schematically shown in figure 2 of Waltham and Lu (2007, p. 15). Plug removal may result in a large pulse of water draining out of the sinkhole that may impact downstream water supplies as well as possibly causing some structural damage. Modeling sinkhole drainage can provide some insights into the sinkhole functioning and perhaps lead to better management of sinkholes in terms of stormwater management.

2.1. Swallet-Capacity Determination

The most important aspect of a sinkhole, from a hydrogeological perspective, is swallet capacity of the sinkhole (Milanović, 2004, p. 22). Determination of swallet capacity is the subject of a detailed discussion in Bonacci (1987, p. 109–115) because poor swallet drainage often results in massive flooding problems when swallet capacities are exceeded (see figure 5.8, p. 108 in Bonacci, 1987). Loss of life, serious injury and displacement, and damage to homes and other structures often occur as a result of flooding in karstic terranes (Day, 2007). As explained in Bonacci, the swallet capacity q depends on the water level h in the pre-swallet retention only when flow in the underlying main karst channel is not under pressure; when under pressure the swallet capacity is dependent on head differences. Swallet drainage is defined by Torricelli's theorem (Streeter and Wylie, 1979, p. 104) according to

$$q(h) = a\pi c_0\sqrt{2gh} \tag{1}$$

which states that water flows out of a wide basin with a velocity that suggests its parts had descended from a height h of the water surface to a level of outflow that is free of pressure losses and assumes no friction which would likely be insignificant anyway for small flow velocities (Bögli, 1980, p. 88). The discharge coefficient c_0 represents the ratio of the actual discharge to that computed from the full area a of the opening and the ideal velocity (Schoder and Dawson, 1934, p. 130). Bonacci (1987) used Equation (1) and other equations to provide a general estimate of the swallet capacity of various sinkholes. However, extensive piezometric measurements are required.

2.2. Theory of Sinkhole Drainage

Drainage of a flooded sinkhole via a swallet will be by point vortex flow which can be quite complicated. Pozrikidis (2001) provides a comprehensive theoretical discussion of vortex motion in various chapters (Pozrikidis, 2001, e.g., p. 288–295 and p. 548–605) although there are entire books devoted to the subject (see for example, Ogawa, 1993; Majda and Bertozzi, 2008). Using the methods described in Pozrikidis (2001, p. 548–558) a visual representation and the counterclockwise velocity field created by a point vortex representing the swallet of a symmetrical circular sinkhole and/or symmetrical elliptical sinkhole may be displayed as shown in Figure 2.

For those instances in which the swallet is offset from the center of the sinkhole (Figures 2(b) and 2(d)), a velocity field and its image may be calculated at any point within the vortex. The velocity field was calculated at the tip of the arrow depicting the counterclockwise vortex flow shown in Figures 2(b) and 2(d). The negative velocity field values are not incorrect because a velocity field is also a velocity vector. Rather the velocity values relate to the direction and nature of the velocity field effect on the counterclockwise flow induced by the primary point vortex centered over the swallet.

In the case of a circular sinkhole (Figures 2(a) and 2(b)) the velocity induced by the image point vortex at the location of the primary vortex may be calculated as the latter rotates around the center of the sinkhole in the direction of the polar angle θ measured around the center of the sinkhole in the counterclockwise direction (Pozrikidis, 2001, p. 558). For the case of a circular sinkhole with a centered swallet (Figure 2(a)), the dimensionless velocity $v_\theta = 0$ whereas for the case of a circular sinkhole with an offset swallet (Figure 2(b)), the dimensionless velocity $v_\theta = 0.0756$.

2.2.1. Sinkhole Flooding Sinkholes, whether naturally occurring or anthropogenic in origin, have a specific capacity to drain water that is sometimes exceeded. When a sinkhole becomes plugged or the underlying solution conduit's capacity to transmit water is exceeded, the ability of a sinkhole to drain all the water being directed into it is exceeded,

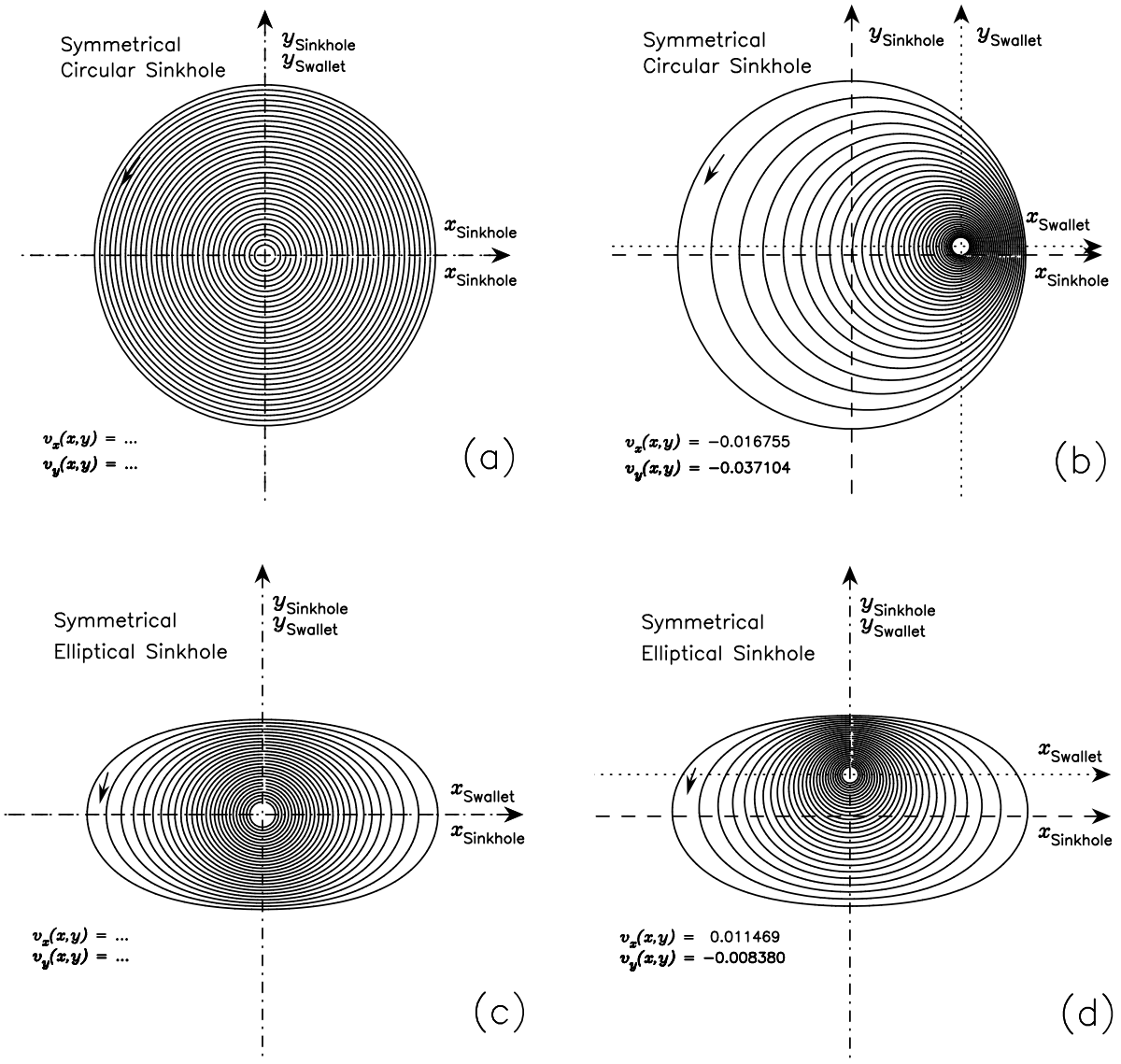

Figure 2. Representative basic sinkhole forms displaying counterclockwise point vortex flow centered on the swallet. Dotted lines represent swallet axes and dashed lines represent sinkhole axes. For a noncentered swallet, a velocity field is created throughout the vortex; a representative velocity field is calculated at the tip of the vortex arrow shown. It will be noted that symmetric sinkholes do not need to have the swallet located directly below the center of the sinkhole. Modified from Pozrikidis (1999, p. 54–55).

which results in flooding of the sinkhole and the surrounding area (McCann and Smoot, 1999). White (1989) provides a brief discussion on the statistics of extreme events that is applicable to sinkhole flooding and serves as an introduction to the basic concepts needed to understand the statistics of sinkhole flooding. Such flooding has obvious implications for local communities (see for example, Crawford, 1984; Dinger and Rebmann, 1986; Reeder and Crawford, 1988; Reese et al., 1997) including litigation (Quinlan, 1984).

Many sinkholes are reinforced and/or modified in various ways to enhance the discharge of stormwater down the sinkhole while attempting to minimize the flow of flotsam and jetsam down the sinkhole, although pollutants are much more difficult to constrain. This author has personally observed the flow of treated industrial wastewaters being directed down a concrete-reinforced sinkhole in which a legitimate Underground Injection Control (UIC) (CSN, 2009; USEPA, 2009) permit had been issued (Fig. 3). Should the sinkhole-drainage capacity receiving treated industrial wastewaters be exceeded for some reason, the wastewaters would then be spread throughout the land surface resulting in serious pollution of both the subsurface from the ongoing discharge and the surface from the temporary sinkhole-flood event.

3. Modeling Sinkhole Drainage Using Various Sinkhole Shapes

Sinkholes all have one or more defined swallets at their base that connects the sinkhole with some underlying conduit system for ultimate discharge at a downstream resurgence as depicted in the generic karst aquifer shown schematically in the block diagram in Figure 4. In the center block of Figure 4 a sinkhole is shown receiving diffuse autogenic and concentrated autogenic recharge which drains into a swallet, through a shaft (Flow Type 4 in Figure 4) to a horizontal vadose conduit. A shaft from this horizontal conduit then drains the water to an underlying phreatic conduit.

It is not difficult to envision the sinkhole in the center block in Figure (4 being plugged by soil when it first developed, as a result of new construction, increased catchments, or as a result of back-flooding emerges from conduits impeded by sediment or breakdown downstream of the underlying solution conduit (Waltham et al., 2005, p. 251). As a result of inflows that exceed the sinkhole drainage capacity, or, as a result of a poor repair efforts, the sinkhole backs-up and overflows. In the case of a swallet plug, the plug will restrict but not necessarily prevent water drainage down the swallet. As the water level rises above the sinkhole plug in the swallet, leakage of the water around and through the plug tends to loosen the compacted soil and lubricate the underlying swallet and consequently, a pressure gradient on top of the soil plug develops. Eventually, leakage of water through and around the soil plug and the pressure gradient from the overlying water combine to drive the plug down through the swallet and the flooded sinkhole then rapidly drains through the swallet. Similar leakage and full drainage will occur in the other circumstances advanced here. If water continues entering the sinkhole, then an eventual mass-balance of inflowing water will equal the draining water unless the inflowing water is greater than or less than the rate of outflow.

3.1. Model Description

Simplified theoretical models for drainage down the swallet of a sinkhole can be developed according to the conditions depicted in Figure 5 in which a sinkhole typically ranges in size from 2–100-m-deep, 10–1000-m-in-diameter, and are commonly circular or elliptical in form (Cvijić, 2005, p. 66) as shown in Figure 2. The modeling method described uses flow into and through a funnel (Rostamian, 2009) as an analogue for sinkhole drainage. It should be noted that some of the sinkholes depicted in Figure 5 are not naturally occurring. For example, Figure 5(c) does not commonly occur, but undercutting of sinkhole walls does sometimes occur so it was considered appropriate to include it in the model analysis.

The sinkholes shown in Figure 5 may be classed according to the three main shapes identified by Cvijić (2005, p. 69). Specifically, Cvijić identified well-shaped sinkholes (cylinder-shaped) which conforms to Figures 5(a) and 5(d), which Cvijić regarded as relatively rare (Cvijić, 2005, p. 70). Figure 5(b) generally matches the funnel-shaped sinkholes of Cvijić (2005, p. 69) and Figure 5(f) generally matches the bowl-shaped sinkholes of Cvijić (2005, p. 69). The remaining sinkholes shown (Figures 5(c) and 5(e)) are exaggeration of sinkholes exhibiting undercutting or other factors due to hydrological-, geological-, and/or geomorphological-site conditions.

Referring to the sinkholes depicted in Figure 5 and applying Torricelli's theorem to flow, drainage through the swallet of a sinkhole is directly related to the water level in the sinkhole according to:

$$q(h) = a_0 c_0 \sqrt{2gh(t)} \tag{2}$$

where Equation (2) differs from Equation (1) only with the consideration of the dependence of swallow-hole drainage on water level as a function of time and where

$$a_0 = \pi\, x_0^2 \tag{3}$$

The volume of water $V(t)$ in the sinkhole at time t equals

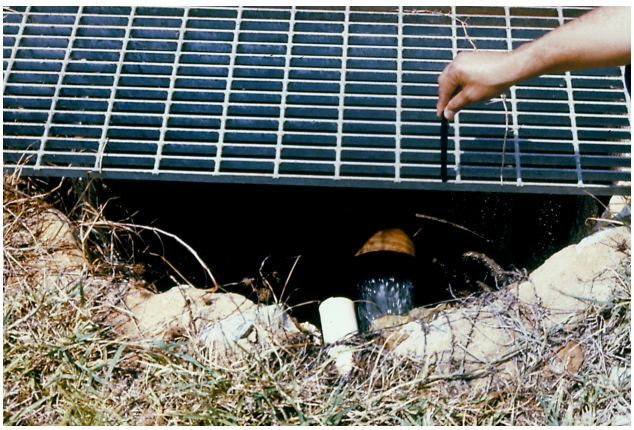

Figure 3. (Left) Restricted access to an improved sinkhole operating as a Class V injection well receiving treated industrial wastewaters at the RCA del Caribe facility, Barceloneta, P.R. (Right) Close-up view of sinkhole depicting concrete reinforcement for improvement of sinkhole sides, and wastewater-discharge pipe draining approximately 500 gpm of treated wastewater from the RCA facility. This Class V Well was operated under Permit No. 83-004 issued by the UIC **Program under the authority of the Federal Safe Drinking Water Act; all facility operations at RCA del Caribe were ceased in 1987 (USEPA, 1994).**

the rate of change according to

$$\frac{dV}{dt} = Q(t) - q(h) \tag{4}$$

Relating dV/dt to water level h in the sinkhole requires recognition of the wetted cross-sectional area $A(h)$ of the sinkhole according to

$$\frac{dV}{dt} = A(h)\frac{dh}{dt} \tag{5}$$

so that Equation (4) now becomes

$$A(h)\frac{dh}{dt} = Q(t) - q(h) \tag{6}$$

An expression for the wetted cross-sectional area $A(h)$ of a sinkhole is relatively easily obtained for a symmetrical cylindrically-shaped sinkhole as depicted in Figure 5(a) that is not dependent on time t or water level h. For a cylindrically-shaped sinkhole (Figure 5(a)), Equation (2) reverts back to Equation (1) and the wetted-cross sectional area of the sinkhole is easily obtained from

$$A = \pi r^2 \tag{7}$$

where r^2 is equivalent to xy and $x = y$ on the circle at the top of Figure 2. For the ellipse shown on the bottom of Figure 2 the area is obtained from

$$A = \pi xy \tag{8}$$

where $y < x$.

An expression for the wetted cross-sectional area $A(h)$ of a symmetrical straight-sided cone-shaped sinkhole or inverted cone-shaped sinkhole, however, is a function of the level of the water level h in the sinkhole (which is a function of time t) and requires use of the equation of a line representing one side of the sinkhole. This is accomplished using the coordinates on the right side of the sinkholes depicted in Figures 5(b) and 5(c).

$$\begin{aligned} y - y_0 &= \left(\frac{y_2 - y_0}{x_2 - x_0}\right)(x - x_0) \\ &= \left(\frac{H}{x_2 - x_0}\right)(x - x_0) \end{aligned} \tag{9}$$

Substituting $h(t)$ for y and solving for $x = r(h)$ yields

$$r(h) = x_0 + \left(\frac{x_2 - x_0}{H}\right)h(t) \tag{10}$$

which represents the radius at a given water level h in the sinkhole at time t so that the wetted cross-sectional area $A(h)$ at time t and water level h may be obtained from

$$A(h) = \pi\left[x_0 + \left(\frac{x_2 - x_0}{H}\right)h(t)\right]^2 \tag{11}$$

For a symmetrical bowl-shaped sinkhole (Figure 5(f)) the wetted cross-sectional area $A(h)$ is much easier to determine as a function of water level h because the radius at a specific water level $r(h)$ may be solved using the equation of a

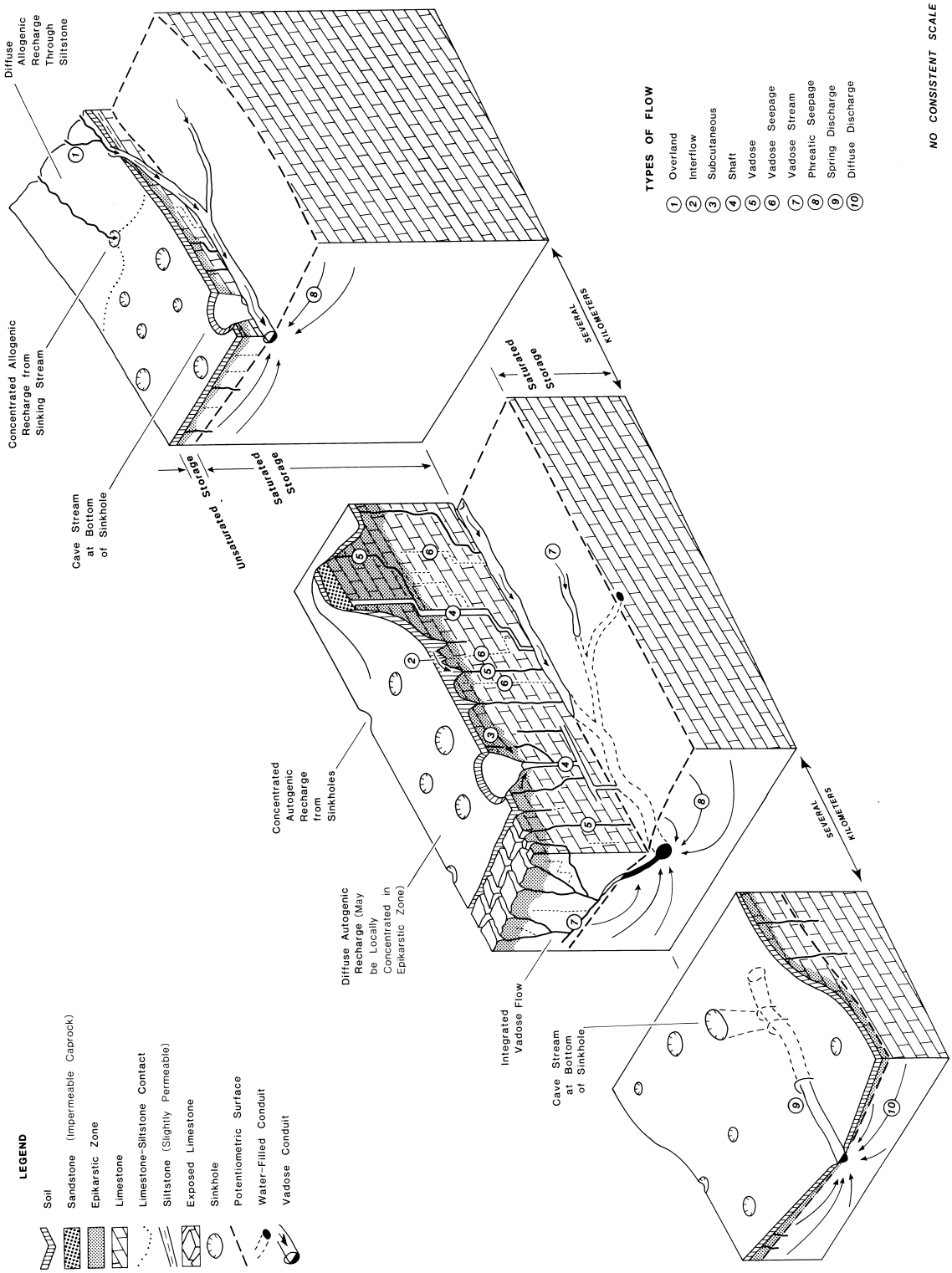

Figure 4. Schematic block diagram depicting the hydrological relationships that exist in a maturely karsted terrane in gently dipping rocks of a low-relief landscape. The cave stream is fed by (1) sinking streams, (2) vertically percolating water infiltrating through soils and sinkholes, (3) tributary cave streams, and (4) seepage through cave walls. Contaminants will enter the aquifer through the same mechanisms that control water inflow (Quinlan, 1989, p. 7).

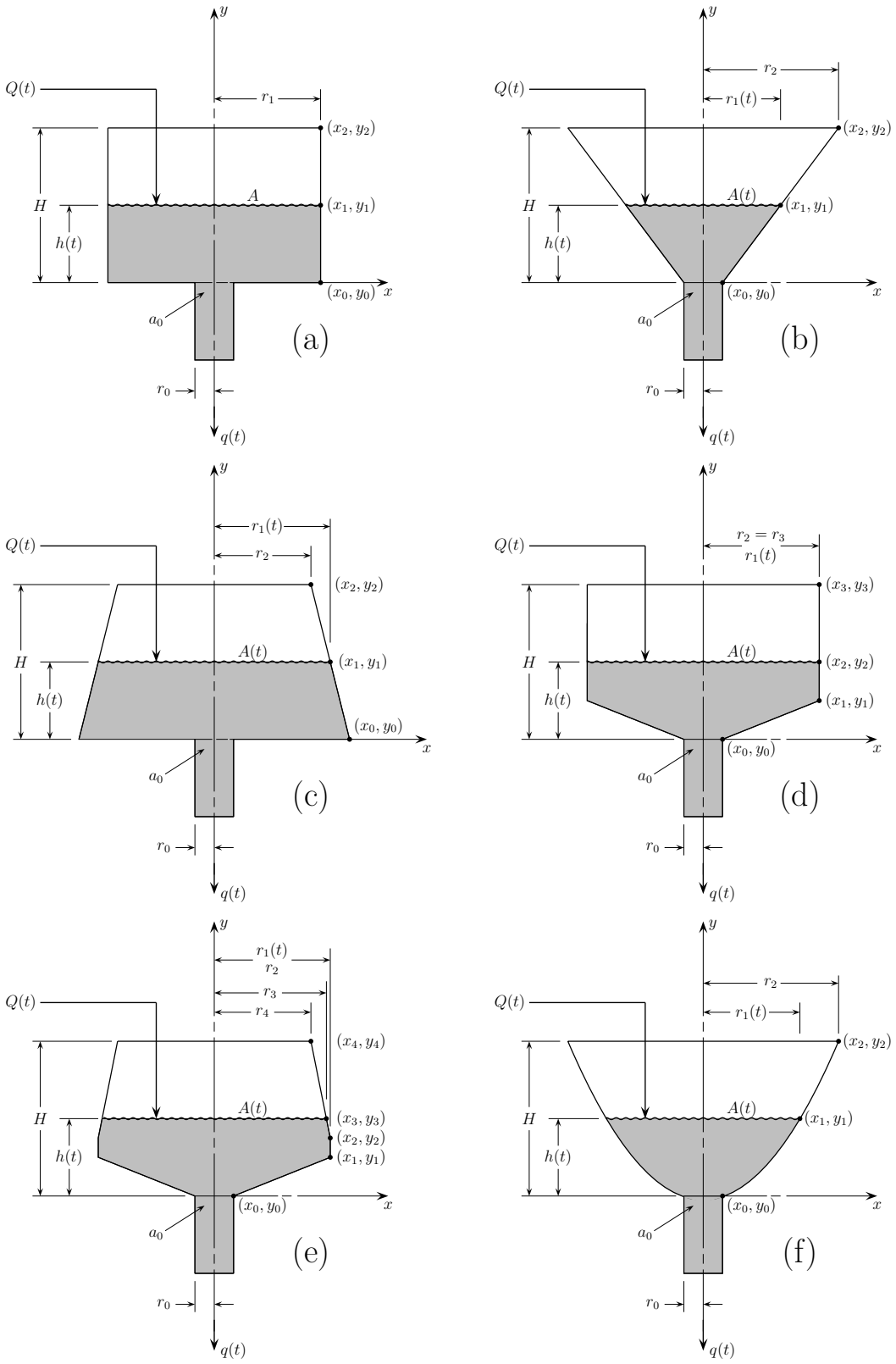

Figure 5. Schematic diagram and coordinate system depicting flow into and out of a sinkhole: (a) symmetrical cylindrically-shaped sinkhole; (b) symmetrical cone-shaped sinkhole; (c) symmetrical inverted-cone-shaped sinkhole; (d) symmetrical cylindrical-cone-shaped sinkhole; (e) combined symmetrical inverted-cylindrical-cone-shaped sinkhole; and (f) symmetrical bowl-shaped sinkhole. Not drawn to representative proportionality.

parabola. The equation for $r(h)$ is then

$$r(h) = \sqrt{\frac{h(t) - bx + c}{a}} \tag{12}$$

and the equation for $A(h)$ becomes

$$A(h) = \pi \left(\frac{h(t) - bx + c}{a} \right) \tag{13}$$

where a, b, and c are constants and a is necessarily positive. Equations (12) and (13) may be simplified by setting $a = 1$ and $b = c = 0$. Equations (9)–(13) are applicable to sinkholes of circular form and are also applicable to sinkholes of elliptical form after minor modifications.

For the case of an asymmetrical sinkhole, the cross-sectional area calculation must be based on a polygon that represents the shape of the asymmetrical sinkhole. This can be accomplished, but no specific equation may be used to represent the shape of the sinkhole and a new polygon would need to be developed for each water-level change Δh.

The appropriate model for sinkhole drainage for each of the various sinkhole shapes shown in Figure 5 is listed in Table 1. Equations (6) and (7) constitute the entire sinkhole drainage model for a symmetrical cylindrically-shaped sinkhole (Figure 5(a)). Equations (6) and (11) constitute the entire sinkhole drainage model for a symmetrical cone-shaped sinkhole and for an inverted cone-shaped sinkhole (Figures 5(b) and 5(c)). Equations (6) and (13) constitutes the entire sinkhole drainage model for a symmetrical bowl-shaped sinkhole (Figure 5(f)). Figures 5(d) and 5(e) are special cases using various combinations of Equations (6), (7), and (11).

Table 1. Drainage models for the sinkhole shapes shown in Figure 5.

Sinkhole Shape	Drainage Model
Cylindrically-Shaped	Equations (6), (7)
Cone-Shaped	Equations (6), (11)
Inverted Cone-Shaped	Equations (6), (11)
Cylindrical-Cone-Shaped	Equations (6), (7), (11)
Inverted-Cylindrical-Cone-Shaped	Equations (6), (7), (11)
Bowl-Shaped	Equations (6), (13)

3.1.1. Critical Inflow rate A critical inflow rate Q_c for a sinkhole may be defined as the rate of inflow that maintains a fully filled sinkhole but which does not overflow. For a fully filled sinkhole that is not overtopped, $h(t) = H$ and the depth of the sinkhole is not increasing (e.g., due to additional geomorphological processes), $dh/dt = 0$, $dV/dt = 0$, and $Q_c = q(h) = 0$. The critical inflow rate Q_c can then be obtained from

$$Q_c = a\pi c_0 \sqrt{2gH} \tag{14}$$

Table 2. Parameters for modeling the various circular sinkhole shapes depicted in Figure 5.

Parameter	Value	Unit
Sinkhole Factors		
Sinkhole Height	6.00	m
Sinkhole Radius	3.00	m
Swallet Factors		
Swallet Height	0.00	m
Swallet Radius	0.10	m
Coef. of Discharge	0.61	
Initial Conditions		
Water Level	3.00	m
Inflow Rate Q;[a] [b]		
$Q \gg q$	0.240	$m^3\ s^{-1}$
$Q > q$	0.190	$m^3\ s^{-1}$
$Q = q$	0.147	$m^3\ s^{-1}$
$Q \ll q$	0.020	$m^3\ s^{-1}$

[a] Model simulations were conducted with four selected initial inflow rates to reflect the specific chosen conditions.

[b] Critical inflow rate $Q_c = 0.208\ m^3\ s^{-1}$ for the sinkhole parameters used here.

Equation (14) is just a slight modification of Equation (1) because water level is not changing. Estimating critical inflow rate can be useful for assessments of the potential for flooding hazards when designing stormwater drainage into existing on-site or nearby sinkholes.

4. Model Simulations

Inflow rates into the sinkholes depicted in Figure 5 is a prime controlling force on sinkhole drainage rate, but not the sole controlling force. This is because the rate of outflow is strongly dependent on the water level h in the sinkhole and the wetted cross-sectional area $A(h)$ of the sinkhole as a function of time t, all of which are a function of sinkhole shape.

Parameters for a moderately-sized circular sinkhole are shown in Table 2. Initial inflow rates for the sinkholes were 0.240, 0.190, 0.147, and $0.020\,m^3\ s^{-1}$. These four inflow rates were chosen to reflect conditions of extreme inflow exceedance ($Q \gg q$), inflow exceedance ($Q > q$), inflow equality ($Q = q$), and extreme inflow inferiority ($Q \ll q$), all relative to outflow.

4.1. Uniform Inflow Rates into the Sinkholes

Uniform inflow into sinkholes does not necessarily translate into a uniform outflow or drainage rate down the swallet at the base of the sinkhole; other hydrological and geological factors not addressed here are also of importance. The model developed in this paper was initially tested using the listed series of four uniform inflow rates. Inflow rates chosen reflect the influence that inflow has on drainage rate while still allowing the initial static water level h in the sinkholes to respond over time as a result of the swallet either being overwhelmed or underwhelmed by the inflowing water.

4.1.1. Uniform Inflow — Water-Level Changes Simulation results for water level Δh as a function of time t for a uniform inflow of water into the sinkholes depicted in Figure 5 are shown in Figure 6. From Figure 6 it can be seen that the water level h in all of the sinkholes depicted in Figure 5 varies significantly and rapidly with respect to time t as water drains through the underlying swallet. Inflow rates that exceed the outflow rate (0.240 and $0.190\,\mathrm{m^3\,s^{-1}}$) both rise rapidly in all the model sinkholes. However, an inflow rate of $0.240\,\mathrm{m^3\,s^{-1}}$ rises extremely rapidly and exceeds the top of the sinkhole to result in overland flooding. The height of the water rise above the sinkhole for an inflow rate of $0.240\,\mathrm{m^3\,s^{-1}}$ could significantly influence the rate of outflow if there is sufficient barriers to the spread of water above the sinkhole which would force ponding and a greater pressure head. Figures 6(c) and 6(e) exhibit a slower rise in water level which is a result of the decreasing cross-sectional area A as a function of increasing water level h (see Figures 5(c) and 5(e)).

For an inflow rate much less than the drainage capacity ($0.020\,\mathrm{m^3\,s^{-1}}$), the water level h drops rapidly with respect to time t. Figures 6(c) and 6(e) exhibit decreasing water levels that differ from the other model sinkhole plots; Figure 6(c) reflects a smoothly decreasing water level that results from the increasing cross-sectional area A as a function of changing water level Δh whereas Figure 6(e) exhibits a mild hump in the decreasing water level which reflects the change in cross-sectional area A as a function of changing water level Δh (see Figure 5(c) and 5(e)).

As expected, for the special case of $Q = q$ $\left(0.147\,\mathrm{m^3\,s^{-1}}\right)$ no apparent change in water level occurs. This is a crucial value for sinkhole drainage because it reflects the transition from $Q < q$ to one of $Q > q$ and should elicit concern from stormwater managers when this rate is being exceeded, because the sinkhole will now begin filling and may be approaching the critical inflow rate.

In terms of sinkhole shapes, it is interesting to note the similarity between all the plots shown in Figure 6. There are some readily apparent minor differences, but overall the plots all reflect the same basic behavior.

4.1.2. Uniform Inflow — Sinkhole Drainage Rate Drainage rate q for uniform inflow rates with respect to t is shown in Figure 7. The plots shown in Figure 7 appear similar to those shown in Figure 6. In each plot, each inflow rate reflects the importance of water level h in the sinkhole. As water level h changes, drainage rate changes accordingly as expected from Equation (2). Also, from Figure 7 it can be noted that an inflow rate of $0.020\,\mathrm{m^3\,s^{-1}}$ becomes asymptotic with the x-axis as expected from Equation (6). An inflow rate less than $0.020\,\mathrm{m^3\,s^{-1}}$ results in complete drainage of the sinkhole (i.e., $h = 0$).

4.1.3. Uniform Inflow — Cross-Sectional Area The cross-sectional areas for uniform inflow rates developed from the simulations are shown in Figure 8 which strongly reflects the various shapes of the different sinkholes shown in Figure 5. Figures 8(a) and 8(d) mostly display a static cross-sectional area for the four different inflow rates. However, for an inflow rate of $0.020\,\mathrm{m^3\,s^{-1}}$, the cross-sectional area rapidly drops to near zero because this particular inflow rate is the only flow rate that is low enough such that the water level in the sinkhole decreases to that part of the sinkhole that becomes cone shaped (0.9 m).

The cross-sectional areas for the cone- and bowl-shaped sinkholes (Figures 5(b) and 5(f)) plots (Figures 8(b) and 8(f)) are very similar and appear similar to the shape of the curves depicted in Figures 6(b) and 8(f), respectively. These plots help emphasize the relationship to cross-sectional area to water level.

The cross-sectional areas plots shown in Figures 6(c) and 6(e) appear very strange and reflect the less uniform sinkhole shapes shown in Figures 5(c) and 5(e). Figure 5(c) is an inverted cone so cross-sectional area increases as water level decreases which causes an inverse response with respect to inflow rate (i.e., increasing inflow rate results in decreasing cross-sectional area). The same effect does not occur for the sinkhole shown in Figure 5(e); rather, the cross-sectional area of the sinkhole increases at first and then rapidly falls to zero. This only occurs with the lowest inflow rate because this is the only inflow rate that results in a water level that decreases to an elevation where the change in sinkhole shape is influences cross-sectional area. The flattening of the $0.240\,\mathrm{m^3\,s^{-1}}$ indicates that the top of the sinkhole had been breached after about 1500 s.

4.2. Varying Inflow Rates into the Sinkholes

Typical inflow rates would not be expected to be uniform as was considered in the previous simulation. Table 3 depicts an increasing and then decreasing inflow rate into the sinkholes. Although the increasing inflow rates and then de-

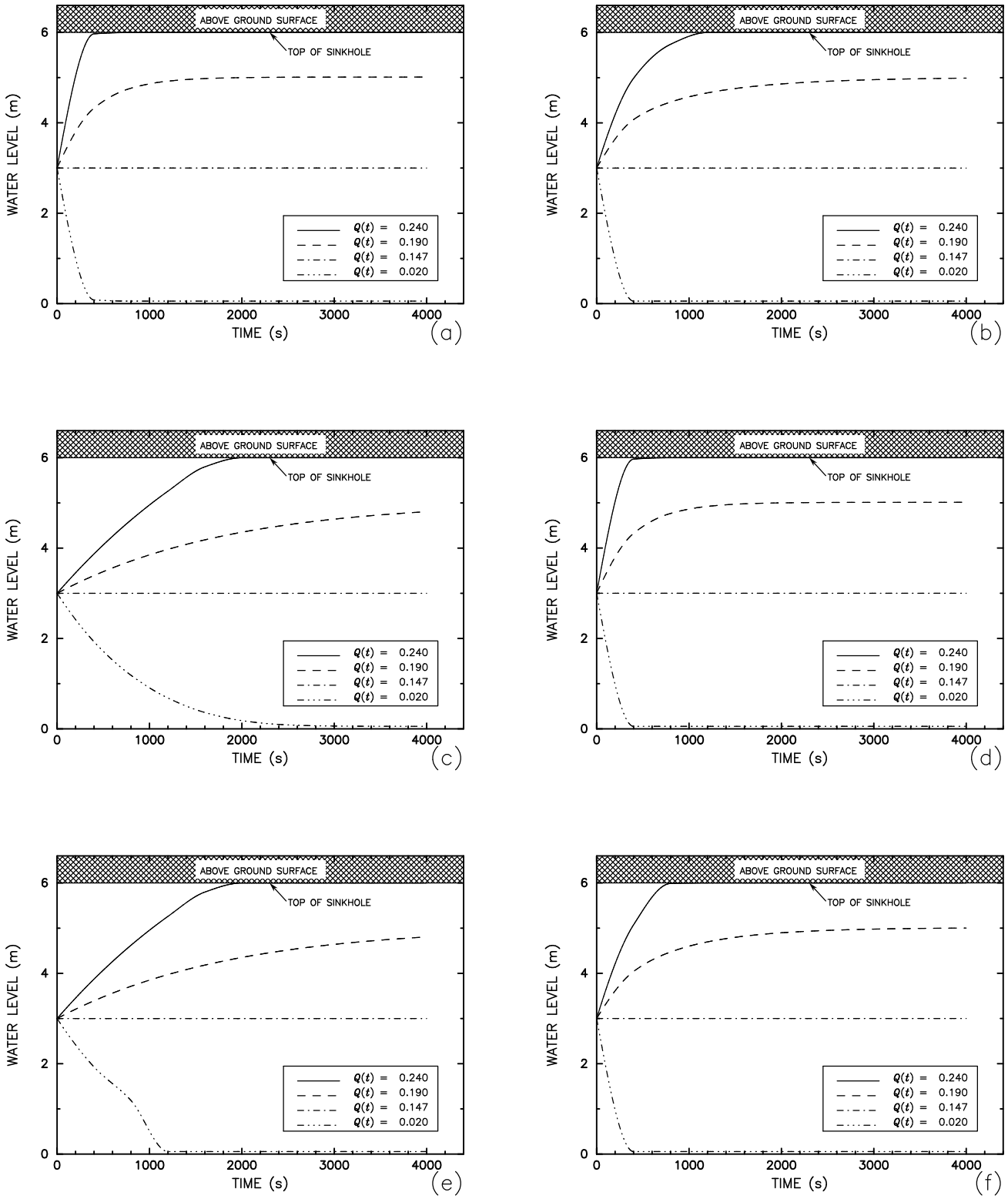

Figure 6. Graphic plots of calculated water level for each of the six types of sinkhole depicted in Figure 5 for uniform inflow rates: (a) symmetrical cylindrically-shaped sinkhole; (b) symmetrical cone-shaped sinkhole; (c) symmetrical inverted-cone-shaped sinkhole; (d) symmetrical cylindrical-cone-shaped sinkhole; (e) combined symmetrical inverted-cylindrical-cone-shaped sinkhole; and (f) symmetrical bowl-shaped sinkhole.

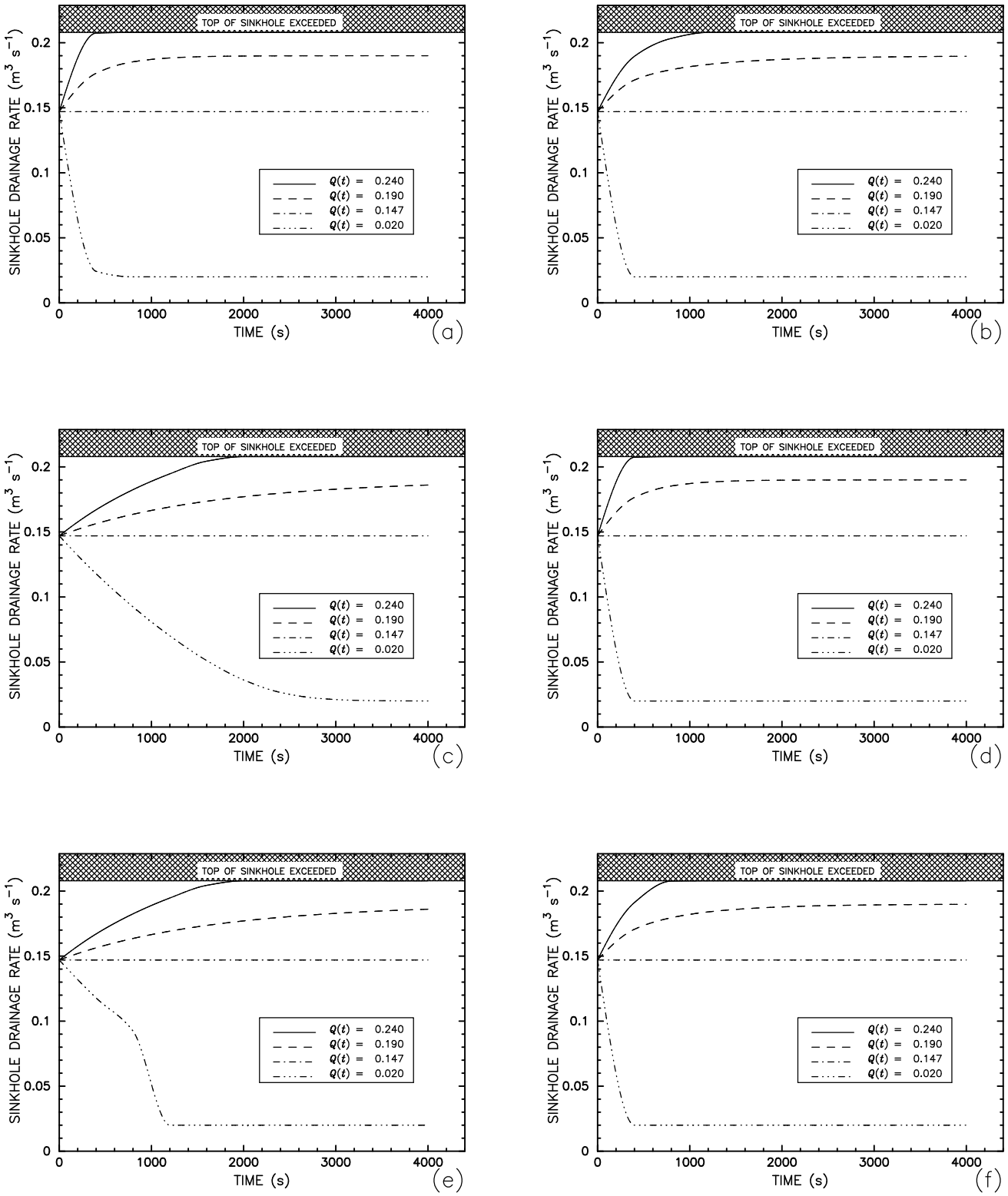

Figure 7. Graphic plots of calculated drainage rate for each of the six types of sinkholes depicted in Figure 5 for uniform inflow rates: (a) symmetrical cylindrically-shaped sinkhole; (b) symmetrical cone-shaped sinkhole; (c) symmetrical inverted-cone-shaped sinkhole; (d) symmetrical cylindrical-cone-shaped sinkhole; (e) combined symmetrical inverted-cylindrical-cone-shaped sinkhole; and (f) symmetrical bowl-shaped sinkhole.

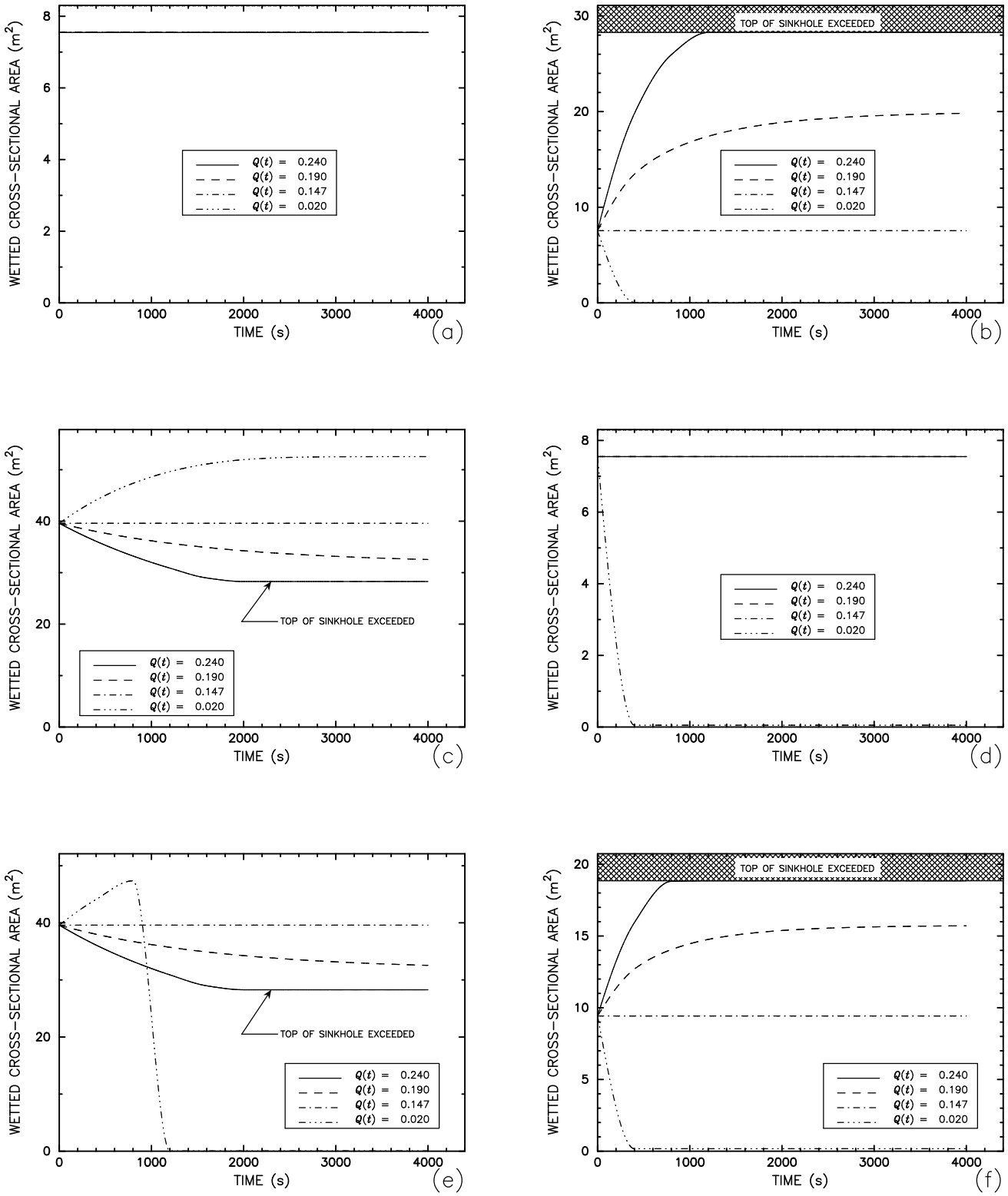

Figure 8. Graphic plots of calculated wetted cross-sectional area for each of the six types of sinkholes depicted in Figure 5 for uniform inflow rates: (a) symmetrical cylindrically-shaped sinkhole; (b) symmetrical cone-shaped sinkhole; (c) symmetrical inverted-cone-shaped sinkhole; (d) symmetrical cylindrical-cone-shaped sinkhole; (e) combined symmetrical inverted-cylindrical-cone-shaped sinkhole; and (f) symmetrical bowl-shaped sinkhole.

Table 3. Increasing and then decreasing inflow rates used to model sinkhole drainage.

Time, s	Inflow Rates, Q_0, $m^3\,s^{-1}$			
	$Q \gg q$	$Q > q$	$Q = q$	$Q \ll q$
0[a]	0.240	0.190	0.147	0.020
400	0.246	0.193	0.149	0.023
800	0.250	0.196	0.150	0.027
1200	0.254	0.199	0.152	0.030
1600	0.258	0.202	0.154	0.033
2000	0.262	0.205	0.155	0.037
2400	0.250	0.200	0.153	0.032
2800	0.237	0.194	0.149	0.028
3200	0.229	0.189	0.146	0.025
3600	0.221	0.185	0.143	0.021
4000	0.213	0.180	0.140	0.018

[a] Zero time represents initial inflow rates.

creasing inflow rates shown in Table 3 are relatively simple, this simulation serves to illustrate the effects of varying inflow rates.

4.2.1. Varying Inflow — Water-Level Changes The water levels shown in Figure 9 show the effect of first increasing and then decreasing inflow rates. In general, these curves are similar to those shown in Figure 6, but with some apparent differences. For example, two of the six sinkholes depicted in Figure 5 show the water level for the greatest inflow rate $\left(0.240\,m^3\,s^{-1}\right)$ exceeding the top of the sinkhole but then falling below the top of the sinkhole as the inflow rate decreases. This also occurs for the $0.190\,m^3\,s^{-1}$ inflow rate for four of the six sinkholes.

For initial inflow rates of 0.147 and $0.020\,m^3\,s^{-1}$, water levels may be observed to fluctuate as expected. In general, the water levels can be observed to initially increase for the $0.147\,m^3\,s^{-1}$ inflow rate and then decrease as expected. However, for the $0.020\,m^3\,s^{-1}$, other than for the inverted sinkhole (Figure 5(c)), the water levels initially fall significantly, then rise, and then begin declining slightly. Only the inverted sinkhole exhibits a smooth and steady decline for the $0.020\,m^3\,s^{-1}$ inflow rate (Figure 9(c)).

4.2.2. Varying Inflow — Sinkhole Drainage Rate As would be expected, the appearance of the drainage rate plots (Figure 10) generally mimics the appearance of the varying water level plots (Figure 9). This occurs because of the defined relationship between water level and drainage rate.

4.2.3. Varying Inflow — Cross-Sectional Area Simulation plots of cross-sectional area A with respect to time t emphasize the importance of sinkhole shape in the model. Figures 11(a) and 11(d) exhibit no change in cross-sectional area because Figures 11(a) and 11(d) are both mostly cylindrically shaped; Figure 11(d) varies near the bottom of the sinkhole, but below the lowest calculated water level. Because inflow rate initially increases, the rate of decrease is insufficient within the allotted time (t = 4000 s) for water level to fall to the elevation where the sinkhole changes to cone shaped in Figure 11(d).

Cone- and bowl-shaped sinkholes (Figure 5(b) and 5(f)) exhibit similarly shaped erratic cross-sectional areas (Figures 11(b) and 11(f)). For the extreme inflow rates $Q > q$ it can be seen in Figures 11(b) and 11(f) that the maximum cross-sectional areas were exceeded because the top of the sinkhole was exceeded in each instance. However, for the $0.190\,m^3\,s^{-1}$ inflow rate the plots also shows that once the water level falls below the top of the sinkhole, the cross-sectional area again falls within the allowable range.

5. Conclusions

Stormwater flow to and drainage down sinkhole swallets occur naturally and anthropogenically. In many instances, stormwater is deliberately directed to sinkholes for drainage as a convenient method for stormwater management. Although many communities have or are beginning to recognize that directing excess stormwater to sinkholes can have serious implications in terms of increased sinkhole development hazard and/or decreased water quality, the practice still continues in many places. In fact, some ordinances even mandate the practice with appropriate controls.

Unfortunately, although directing excess stormwater to sinkholes for drainage has long been practiced and still occurs in some instances, no real guidance exists for determining and understanding sinkhole functioning in terms of drainage. This paper presents a basic introduction into the sinkhole functioning by explaining the significance of point vortex flow and developing some simple models for drainage simulations to be conducted

The simulations illustrate, for the selected example sinkholes and the chosen dimensions, the sensitivity of the swallets to varying inflow rates. Drainage rate is shown to be primarily a function of water level in the sinkhole, but also as a function of sinkhole shape, cross-sectional area, swallet diameter, and time.

The significance of sinkhole and swallet dimensions for sinkhole drainage emphasizes the need to take careful measurements of the basic hydrologic and geologic parameters so that drainage capabilities of the sinkhole may be reasonably estimated. Such an estimate will not necessarily lead to inflow restrictions that will prevent expansion of the sinkhole or new sinkhole development. However, minimization of sinkhole-flooding hazard may be achieved if sinkhole-drainage capacity and functioning is reasonably well under-

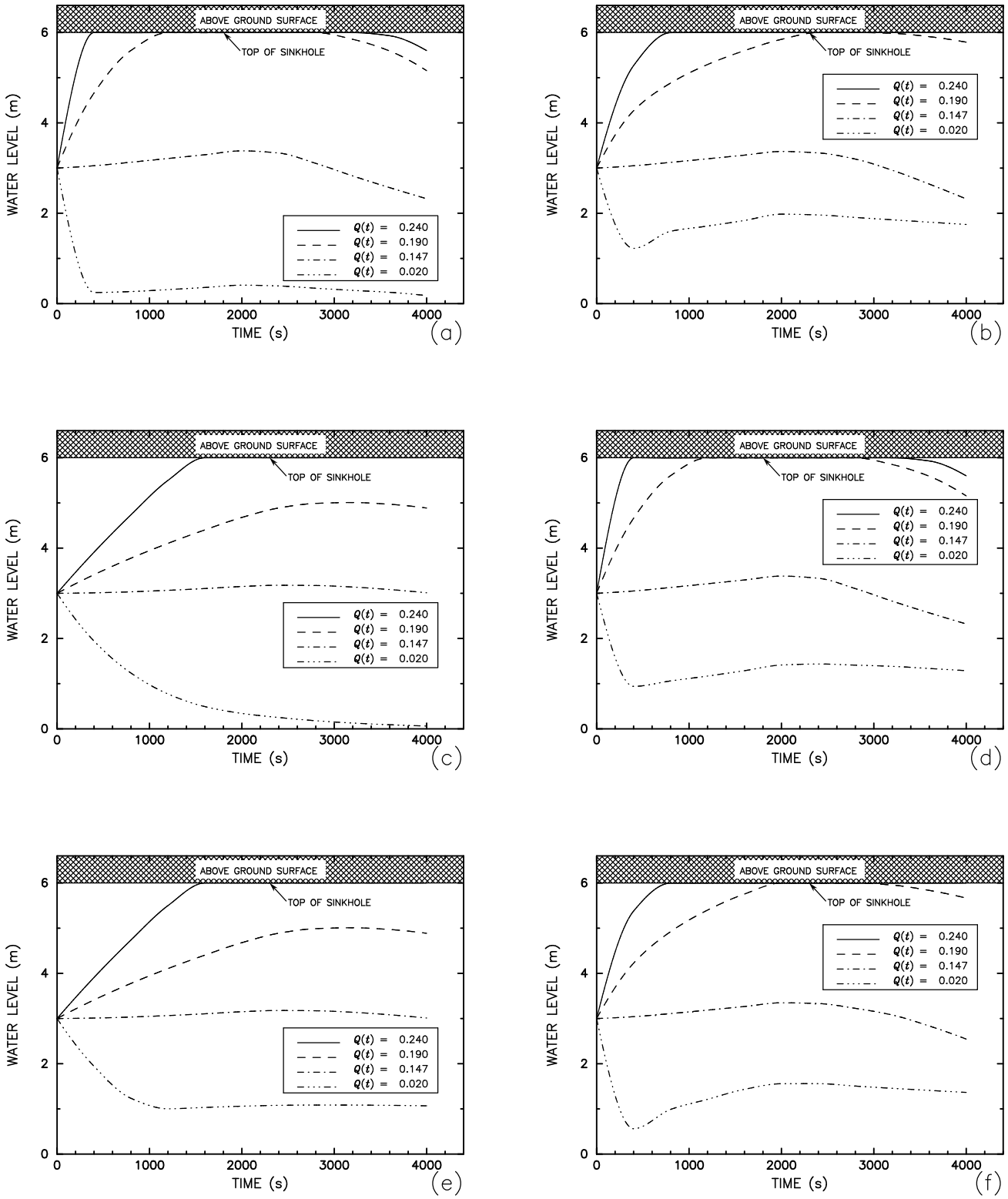

Figure 9. Graphic plots of calculated water level for each of the six types of sinkhole depicted in Figure 5 for varying inflow rates: (a) symmetrical cylindrically-shaped sinkhole; (b) symmetrical cone-shaped sinkhole; (c) symmetrical inverted-cone-shaped sinkhole; (d) symmetrical cylindrical-cone-shaped sinkhole; (e) combined symmetrical inverted-cylindrical-cone-shaped sinkhole; and (f) symmetrical bowl-shaped sinkhole.

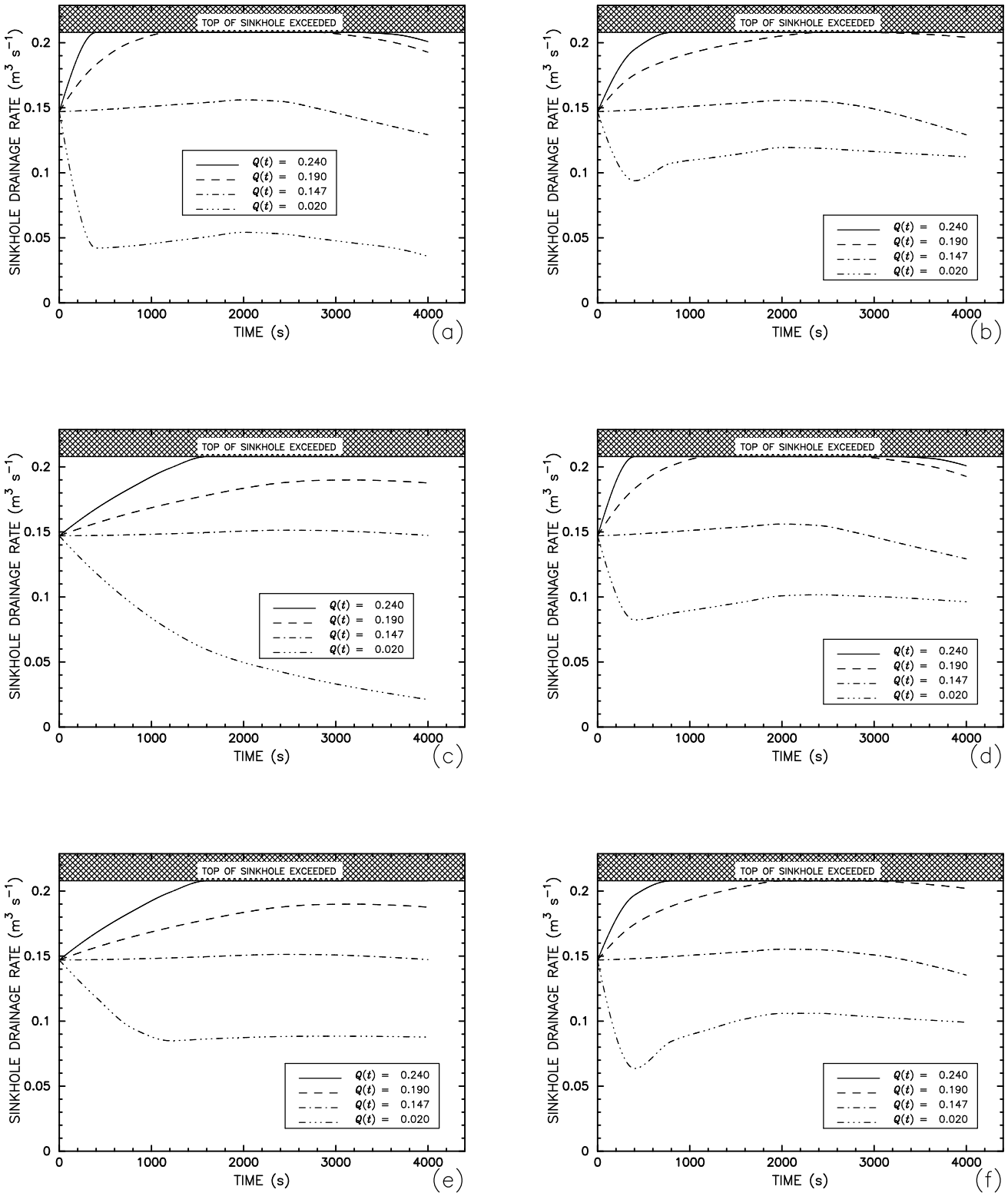

Figure 10. Graphic plots of calculated outflow drainage rate for each of the six types of sinkholes depicted in Figure 5 for varying inflow rates: (a) symmetrical cylindrically-shaped sinkhole; (b) symmetrical cone-shaped sinkhole; (c) symmetrical inverted-cone-shaped sinkhole; (d) symmetrical cylindrical-cone-shaped sinkhole; (e) combined symmetrical inverted-cylindrical-cone-shaped sinkhole; and (f) symmetrical bowl-shaped sinkhole.

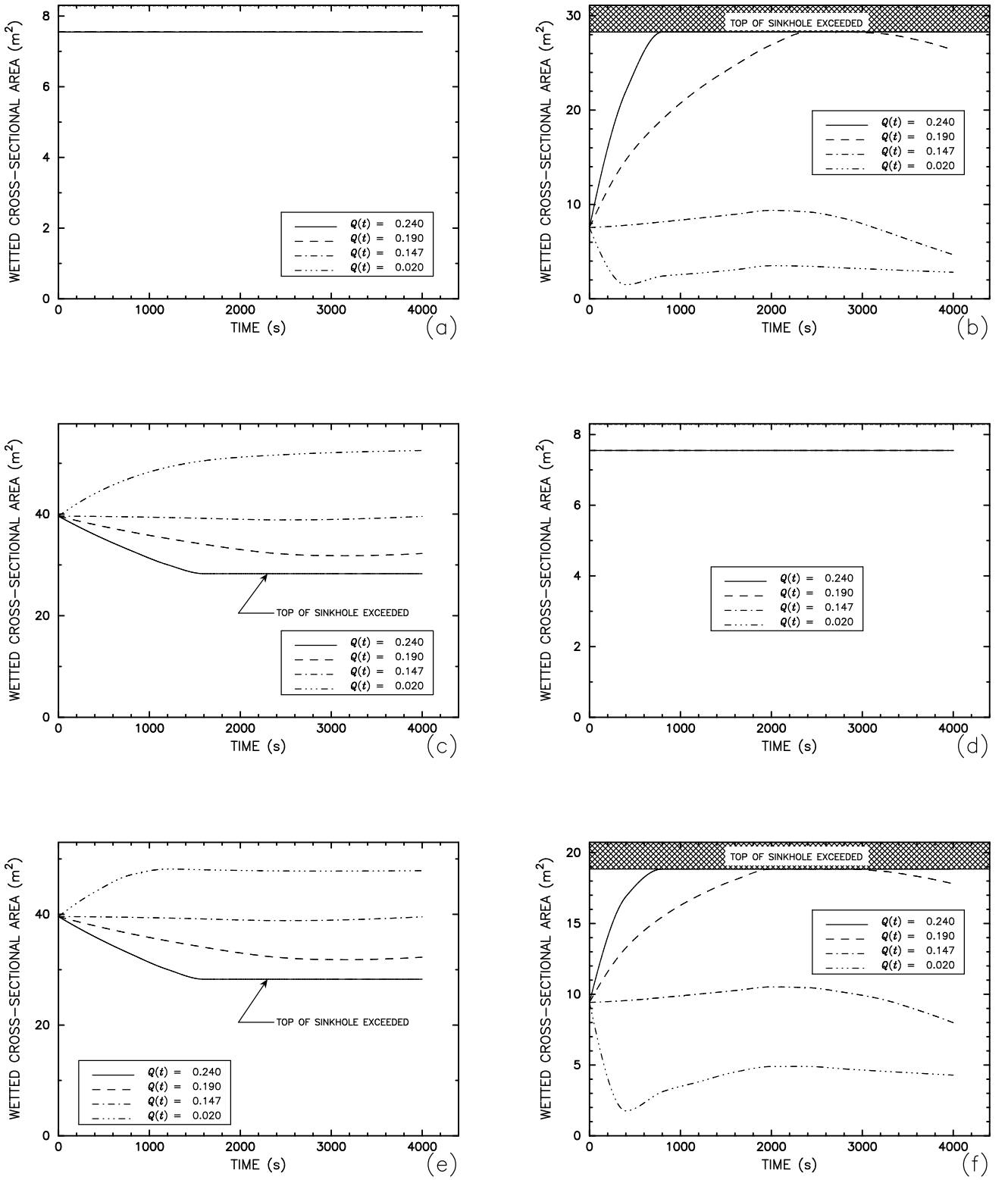

Figure 11. Graphic plots of calculated wetted cross-sectional area for each of the six types of sinkholes depicted in Figure 5 for varying inflow rates: (a) symmetrical cylindrically-shaped sinkhole; (b) symmetrical cone-shaped sinkhole; (c) symmetrical inverted-cone-shaped sinkhole; (d) symmetrical cylindrical-cone-shaped sinkhole; (e) combined symmetrical inverted-cylindrical-cone-shaped sinkhole; and (f) symmetrical bowl-shaped sinkhole.

stood and appropriate stormwater-management plans implemented.

Acknowledgments

The author would like to thank Dr. William Schiesser of Lehigh University for his advise on the development and numerical solution of the basic sinkhole-model equation. His guidance and assistance over the years are greatly appreciated. I would also like to thank Michael Eller of the U.S. Environmental Protection Agency for his careful review and comments of an early draft of my manuscript.

Notation

A	wetted cross-sectional area of sinkhole [L^2]
a	wetted cross-sectional area of swallow hole [L^2]
a_o	wetted cross-sectional area times π of swallow hole [L^2]
c_0	discharge coefficient, equal to the velocity coefficient times the contraction coefficient []
g	gravitational acceleration [L T^2]
h	height of sinkhole [L]
H	height of sinkhole [L]
Q	inflow rate into the sinkhole from all sources [L^3 T]
Q_c	critical inflow rate into the sinkhole from all sources such that the sinkhole remains fully filled [L^3 T]
q	rate of drainage (discharge) out of the sinkhole [L^3 T]
r_0	swallow hole radius [L]
r_1	radius of sinkhole at water height in sinkhole [L]
r_2	maximum sinkhole radius [L]
V	volume [L^3]
x_i	x (horizontal) coordinates for one side of the sinkhole []
y_i	y (vertical) coordinates for one side of the sinkhole []

Acronyms

UIC Underground Injection Control

References

Barner, W.L., 1999, Comparison of stormwater management in a karst terrain in Springfield, Missouri — case histories: Engineering Geology, v. 52, p. 105–112.

Bögli, A., 1980, Karst hydrology and physical speleology: Berlin, Springer-Verlag, 284 p.

Bonacci, O., 1987, Karst hydrology with special reference to the Dinaric Karst: Berlin, Springer-Verlag, 184 p.

Crawford, N.C., 1984, Sinkhole flooding associated with urban development upon karst terrain: Bowling Green, Kentucky, *in* Beck, B.F., ed., Proceedings of the sinkholes: Their geology, engineering & environmental impact conference: Boston, Mass., A.A. Balkema, p. 283–292.

Crawford, N.C., and Gorves, C.G., 1995, Sinkhole collapse and ground water contamination problems resulting from storm water drainage wells on karst terrain, *in* Beck, B.F., ed., Proceedings of the karst geohazards: Engineering and environmental problems in karst terrane conference: Brookfield, Vt., A.A. Balkema, p. 257–264.

CSN, 2009, Stormwater design guidelines for karst terrainin the chesapeake bay watershed, version 2,0, CSN Technical Bulletin No. 1: Chesapeake, Va., Chesapeake Stormwater Network, Karst Working Group.

Cvijić, J., 2005, Karst: A geographic monograph [Translation of Ph.D. Dissertation (1895) Das Karstphänomen, Versuch einer morphologischen Monographie], *in* Stevanović, Z., and Mijatović, B., eds., Cvijić and karst: Belgrade, Serbia, Serbian Academy of Science and Arts (SASA) and its Board on Karst Hydrology, p. 57–146.

Day, M.J., 2007, Hazards in the karst of Jamaica, *in* Parise, M., and Gunn, J., eds., Natural and anthropogenic hazards in karst areas: Recognition, analysis, and mitigation: London, U.K., The Geological Society of London, p. 173–184, doi:10.1144/SP279.14.

Dinger, J.S., and Rebmann, J.R., 1986, Ordinance for the control of urban development in sinkhole areas in The Blue Grass Region, Lexington, Kentucky, *in* Crawford, N.C., and Quinlan, J.F., eds., Proceedings of the environmental problems in karst terranes and their solutions conference: Dublin, Ohio, National Water Well Association, p. 163–180.

Field, M.S., 1989, The vulnerability of karst aquifers to chemical contamination, *in* Zaporozek, A., ed., Recent advances in ground-water hydrology: Minneapolis, Minn., American Institute of Hydrology (AIH), p. 130–142.

Fleury, S., 2009, Land use policy and practice on karst terrains: Living on limestone: Springer, 187 p., doi:10.1007/978-1-4020-9670-9.

Ford, D., and Williams, P., 2007, Karst hydrogeology and geomorphology: West Sussex, U.K., John Wiley & Sons, Ltd, 562 p.

Ford, D.C., 1963, Aspects of the geomorphology of the Mendip Hills [Ph.D. thesis]: Oxford, U.K., Oxford University.

Gao, Y., 2002, Karst feature distribution in southeastern Minnesota: Extending GIS-based database for spacial analysis and resource management [Ph.D. thesis]: Minneapolis, University of Minnesota.

Jennings, J.N., 1985, Karst geomorphology: Oxford, U.K., Basil Blackwell, Ltd., 293 p.

Kalmes, A., and Mohring, E., 1995, Sinkhole treatment to improve water quality and control erosion in southeastern Minnesota, *in* Beck, B.F., ed., Proceedings of the karst geohazards: Engineering and environmental problems in karst terrane conference: Brookfield, Vt., A.A. Balkema, p. 265–272.

Keith, J.H., Bassett, J.L., and Duwelius, J.A., 1995, Modification of highway runoff quality by sinkhole drainage structures, Highway 37 improvement project Lawrence County, Indiana, *in* Beck, B.F., ed., Proceedings of the karst geohazards: Engineering and environmental problems in karst terrane conference: Brookfield, Vt., A.A. Balkema, p. 273–284.

Majda, A.J., and Bertozzi, A.L., 2008, Vorticity and incompressible flow: Cambridge, U.K., Cambridge University Press, 545 p.

McCann, M.S., and Smoot, J.L., 1999, A review of stormwater best management practices for karst areas, *in* Beck, B.F., Pettit, A.J., and Herring, J.G., eds., Proceedings of the hydrogeology and engineering geology of sinkholes and karst–99 conference: Brookfield, Vt., A.A. Balkema, p. 395–398.

MDE, 2000, Maryland stormwater design manual: Baltimore, Maryland Department of the Environment, URL `http://www.mde.state.md.us/Programs/WaterPrograms/SedimentandStormwater/stormwater_design/index.asp`, [accessed June 17, 2009].

Milanović, P.T., 2004, Water resources engineering in karst: Boca Raton, Fla., CRC Press., 312 p.

MPCA, 2008, The Minnesota stormwater manual: Minneapolis-St. Paul, Minnesota Pollution Control Agency, URL `http://www.pca.state.mn.us/publications/wq-strm9-01.pdf`, [accessed June 17, 2009].

Ogawa, A., 1993, Vortex flow: Boca Raton, Fla., CRC Press, 311 p.
Parizek, R.R., 2005, Opportunities to enhance management of karstic aquifers, *in* Stevanović, Z., and Mijatović, B., eds., Water resources & environmental problems in karst: Belgrade, Serbia, Serbian Academy of Science and Arts (SASA) and its Board on Karst Hydrology, p. 231–238.
Pozrikidis, C., 1999, Little book of streamlines: San Diego, Academic Press, 148 p.
Pozrikidis, C., 2001, Fluid dynamics: Theory, computation, and numerical simulation: Boston, Kluwer Academic Publishers, 675 p.
Quinlan, J.F., 1984, Litigious problems associated with sinkholes, emphasizing recent Kentucky cases alleging liability when sinkholes were flooded, *in* Beck, B.F., ed., Proceedings of the sinkholes: Their geology, engineering & environmental impact conference: Boston, Mass., A.A. Balkema, p. 293–296.
Quinlan, J.F., 1989, Special problems of ground-water monitoring in karst terranes: Recommended protocols & implicit assumptions, EPA/600/X-89/050 (unpublished draft): Washington, D.C., U.S. Environmental Protection Agency.
Reeder, P.P., and Crawford, N.C., 1988, Urban storm water runoff: Bowling Green, Kentucky, *in* Quinlan, J.F., ed., Proceedings of the second conference on environmental problems in karst terranes and their solutions: Dublin, Ohio, National Water Well Association, p. 69–95.
Reese, A.J., Cantrell, A., and Scarborough, J., 1997, Sinkhole and drainage planning in Johnson City, Tennessee, *in* Beck, B.F., and Stephenson, B., eds., Proceedings of the engineering geology and hydrogeology of karst terranes conference: Brookfield, Vt., A.A. Balkema, p. 265–271.
Rostamian, R., 2009, A funnel with variable inflow rate: Project 1, Math. 481, UMBC, URL `http://www.math.umbc.edu/~rouben/2009-01-math481/proj1-rr.pdf`, [accessed March 21, 2009].
Schoder, E.W., and Dawson, F.M., 1934, Vorticity and incompressible flow: New York, McGraw-Hill Book Company, Inc., 429 p.
Sowers, G.F., 1996, Building on sinkholes: Design and construction of foundations in karst terrain: New York, American Society of Civil Engineers (ASCE) Publications, 202 p.
Streeter, V.L., and Wylie, E.B., 1979, Fluid mechanics: seventh edn., New York, McGraw-Hill Book Co., 562 p.
Sweeting, M.M., 1973, Karst landforms: New York, Columbia University Press, 362 p.
USEPA, 1994, EPA Superfund Record of Decision: RCA del Caribe (EPA ID: PRD090370537), EPA/ROD/R02-94/240: Washington, D.C., U.S. Environmental Protection Agency, URL `http://www.epa.gov/superfund/sites/rods/fulltext/r0294240.pdf`, [accessed June 19, 2009].
USEPA, 2009, Class V Wells: Washington, D.C., U.S. Environmental Protection Agency, URL `http://www.epa.gov/safewater/uic/class5/comply_minrequirements.html`, [accessed June 15, 2009].
Waltham, T., Bell, F.G., and Culshaw, M.G., 2005, Sinkholes and subsidence: Karst and cavernous rocks in engineering and construction: Chichester, U.K., Springer, 382 p.
Waltham, T., and Lu, Z., 2007, Natural and anthropogenic rock collapse over open caves, *in* Parise, M., and Gunn, J., eds., Natural and anthropogenic hazards in karst areas: Recognition, analysis, and mitigation: London, U.K., The Geological Society of London, p. 13–21, doi: 10.1144/SP279.3.
White, E.L., 1989, Flood hydrology, *in* White, W.B., and White, E.L., eds., Karst hydrology, concepts from the Mammoth Cave area: New York, Van Nostrand Reinhold, p. 127–143.
Williams, P.W., 1971, Illustrating morphometric analyses of karst with examples from New Guinea: Zeitschrift für Geomorphologie, v. 15, no. 1, p. 40–61.
Williams, P.W., 1983, The role of the subcutaneous zone in karst hydrology: Journal of Hydrology, v. 61, p. 45–67.
Williams, P.W., 1985, Subcutaneous hydrology and the development of doline and cockpit karst: Zeitschrift für Geomorphologie, v. 29, p. 463–482.
Zhou, W., 2007, Drainage and flooding in karst terranes: Environmental Geology, v. 51, p. 963–973, doi:10.1007/s00254-006-0365-3.

Malcolm S. Field, U.S. Environmental Protection Agency, National Center for Environmental Assessment (8623P), 1200 Pennsylvania, Ave., N.W., Washington, D.C. 20460, USA, e-mail: `field.malcolm@epa.gov`

This preprint was prepared with AGU's LaTeX macros v. 5.01, with a slight modification to the extension package 'AGU^{++}' by P. W. Daly, v. 1.6b from 1999/08/19.